

The Effect of Turbulence on the Aerodynamics of Low Reynolds Number Wings

S. Watkins, S. Ravi, and B. Loxton

Abstract—Tests on 3-D and nominally 2-D airfoils are presented relevant to micro air vehicle (MAV) flight. Thin, pressure-tapped, flat airfoils were testing at a Reynolds number of 75000 under a range of turbulence characteristics. Turbulence intensity was varied from 1.2 to 12.6% and the longitudinal integral length scale was varied from 0.17 to 1.21m. The overall trend when the intensity was increased was to reduce the lift curve slope but increase the maximum lift coefficient. When the length scale was increased and the intensity was held nominally constant, the lift curve slope increased and the maximum lift coefficient reduced. The largest variation in lift with increasing intensity was found at between 5 and 10 degrees where a reduction in lift of up to 28% was found. Spectrograms of the pressure fluctuations gave insight into the behavior of the laminar separation bubble under the influence of turbulence.

Index Terms—MAV, low Reynolds number, aerofoil, turbulence, intensity, scale

I. INTRODUCTION

Micro air vehicles (MAVs) are currently of interest for use in military and civilian operations due to their potential for surveillance and information gathering [1]. Their general role will be to operate where direct line of sight is not available (from either a person or a larger manned, or unmanned, craft) and they will operate at low altitude and usually in complex terrain. MAVs will thus be flown in the lower levels of the turbulent atmospheric boundary layer (ABL) and sometimes within the roughness zone; that is the layer of air close to the ground which contains the local wakes and influences of upstream objects such as buildings. This environment is highly turbulent on days when there is any appreciable atmospheric wind and this turbulence presents a significant challenge to any craft, artificial or natural, operating on all but the calmest of days. Developing an MAV that can maintain a stable sensor platform in any environment on windy days is a challenge, and one that must be overcome if MAVs are to be successfully utilised in the field if their operation is not limited to "fair weather use only". Consequently the environment is emerging as a major constraint on the operations of MAVs with an increasing vulnerability to turbulence as size and speed reduces [2].

Since MAVs have spans of less than one metre and usually fly at speeds of less than 10m/s they operate in a relatively

low Reynolds number range (less than 100,000, see Figure 1). In this range complex flow phenomena exist within the boundary layer. A review paper by Pines et al [3] points to the lack of knowledge of the fundamental flow physics in this régime, which is needed to accurately model the steady and unsteady environments that MAVs encounter during flight.

In smooth flow, the performance of airfoils at Reynolds numbers above 500,000 is well understood; however the performance deteriorates rapidly at Reynolds numbers below 500,000 and is relatively poorly documented Mueller [4]. At these low Reynolds numbers extensive low energy laminar flow can be present resulting in subsequent early separation and sometimes later reattachment (Figure 1) and can result in increased drag and reduced performance. Such phenomena is further complicated when the approach flow is turbulent.

A wide range of turbulent flow conditions is experienced outdoors, due to the wide range of atmospheric wind-speeds, flight speeds and terrain conditions. Discounting extreme climatic conditions the mean atmospheric wind speed can vary from 0 to about 10 m/s and the flight speed of MAVs is similar. Thus the turbulence intensity, as perceived by the MAV, can vary from zero (flying in calm conditions) to infinity (when flying at the mean atmospheric wind speed; essentially hovering with respect to the wind). In our prior work we have documented some of these conditions by a series of outdoor experiments measuring atmospheric turbulence, both in the earth reference frame (i.e. on a mast fixed to the ground) and also by "flying" banks of dynamically responsive probes through a variety of terrains [5]. Here we replicate some of the typical turbulence intensities experienced by MAVs and investigate the influence on a thin flat plate aerofoil.

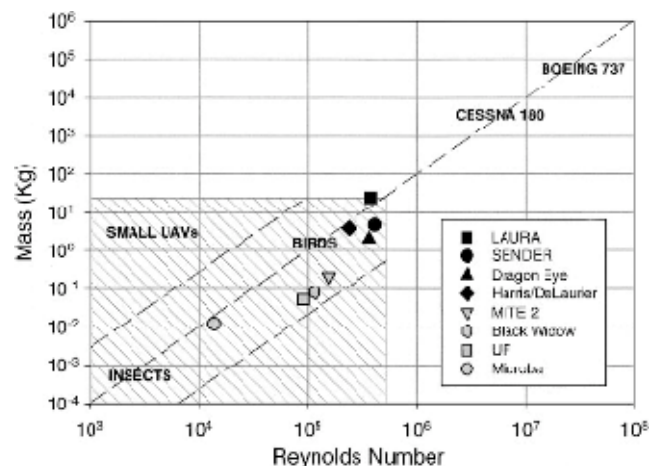


Figure 1 - Relative Reynolds number environment of small UAVs and MAVs. (source: Mueller [4])

Manuscript received March 31, 2010. This work was supported in part by the USAF via the AFOSR Project number 084061: 2008-2009.

Simon Watkins is a Professor in the School of Aerospace, Mechanical and Manufacturing Engineering at RMIT University, Melbourne, Australia. Sridhar Ravi and Ben Loxton are two of his doctoral students. Contact for Simon Watkins: phone +61399256084, fax +61399256108, email simon@rmit.edu.au

The integral length scales of turbulence found in the atmosphere depend upon the terrain and, to a lesser extent, the altitude; but typically they are of the order of 10+m. Replication of such large turbulence scales is unfeasible in wind tunnels and thus wind engineers utilise reduced scale models (e.g. for tests on tall buildings). Since we are interested in studying the combined effects of Reynolds number and turbulence on small airfoils, reduced scaling tests may not be practical. Thus whilst the Reynolds numbers and turbulence intensities can be relatively easily matched, the scales cannot. However some tests performed for this work were conducted in the largest wind tunnel in the Southern hemisphere. This facility enabled much larger integral length scales of turbulence to be generated than have previously been investigated. An overview of the facility including flight testing of fixed wing, rotary wing and flapping MAVs in replicated turbulence can be found in [6].

The work presented here aims to build on the work of smooth flow low Reynolds number aerodynamics by subjecting pressure-tapped airfoils to a range of turbulent flow conditions. A range of turbulence intensities are considered and the effects of different integral length scale are identified, whilst keeping the intensities nominally constant.

II. AEROFOIL AND WIND TUNNELS

In smooth flow testing it is desirable to investigate 2-D flows around airfoils and thus tunnel or CFD tests are undertaken where the aerofoil section is bounded by sidewalls; either real or virtual. When 2-D testing airfoils in turbulent flows (which are inherently three-dimensional), it would seem reasonable to have the lateral boundaries (i.e. sidewalls of the tunnel or perhaps end plates) separated by a distance that is at least equal to the lateral integral length scale. This provides a new constraint which dictates the use of relatively large test domains and complicates experimental testing.

A. Flat Plate Aerofoil

Based on the work of Mueller [4], a thin flat plate aerofoil was selected. This airfoil produces well-documented regions of laminar separation and reattachment at the leading edge. The aerofoil, shown in Figure 2, comprises of a 2% thickness, chord of length 0.150m with a super-elliptical leading edge, and a tapered trailing edge. Due to the fragility and flexibility of the aerofoil it was necessary to use guying threads to avoid excessive vibration. As these were well-removed from the location of the pressure taps the aerodynamic effects were considered negligible, see Figure 3.

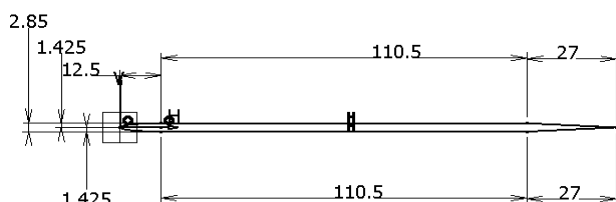


Figure 2 – Airfoil section, all dimensions in mm

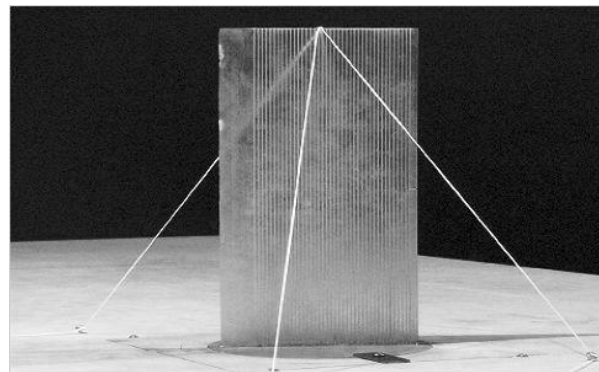


Figure 3 – Prototyped 3-D wing with integral pressure taps.

Wings were manufactured using a rapid prototyping method with integral surface pressure taps. Pressure measurements were made using the Dynamic Pressure Measurement System (DPMS) manufactured by Turbulent Flow Instrumentation (TFI) [7]. This system digitally measures pressure signals on 60 channels. The tapped wing consisted of 40 channels for both 2-D as well as 3-D tests. Tubing of 1mm ID was used to connect the integral pressure taps to DPMS module. For 2-D tests, the tubing length used was 500mm and for 3-D tests the tubing length was 300mm. A (relatively small) dynamic correction was used to enhance the frequency response giving an essentially flat amplitude response to several hundred hertz. This was well above any frequencies of interest (see later). Digital data acquisition was by a National Instruments 6032E DAQ card in a PC.

B. RMIT University Industrial Wind Tunnel

2-D and 3-D testing was performed in the RMIT 2x3x9m closed jet, closed test section Industrial Wind Tunnel (IWT) which was configured to generate turbulence using a series of grids. The turbulence levels generated in the IWT cover much of the range of relative turbulence intensities that a MAV will experience [5]. A distance of greater than 10 times the grid element width is required for the turbulence to become reasonably well mixed and fully homogenous. This requires the model to be located near the end of the test section, about 9m from the grids.

C. Monash University Wind Tunnel

2-D airfoil testing was performed in the Monash University Tunnel. The facility and modifications performed to generate various intensities and integral length scales are detailed in [9] thus only an overview is given here. The facility is sufficiently large to permit flight of MAVs of up to about 1m span. It is driven by two 5-meter diameter, fixed pitch, variable speed, axial fans situated at the start of the lower circuit.



Figure 4 – Pressure tapped wing - 2-D configuration between end plates RMIT IWT

A schematic of the wind tunnel is shown in Figure 5. The wind tunnel is of the closed circuit type, and was designed as a multiple use facility with three working sections: (i) an open-jet automotive aeroacoustic test section on the lower level; (ii) a general purpose high Reynolds number closed test section, also on the lower level and (iii) a wind engineering, closed test section on the upper level.

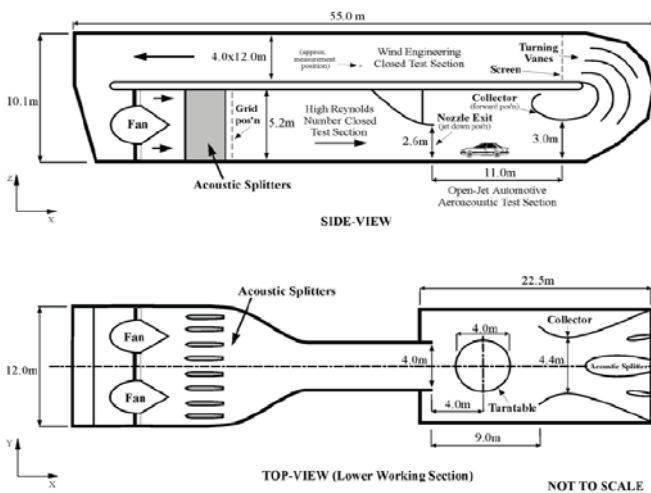


Figure 5 – Monash University Wind Tunnel - Schematic

The open-jet automotive aeroacoustic test section provides a low turbulence level area for testing in relatively smooth air (longitudinal turbulence intensity $\sim 1.5\%$). It also offers the opportunity for MAV flight testing including the ability to fly from the relatively stationary air (in the plenum chamber) into the jet, thus permitting a step change in flight speed – from either side of the jet, or from above.

As the focus of our work is to understand the effects of turbulence the majority of tests were carried out in the wind engineering section on the upper level of the tunnel. This has a 4-meter high by 12-meter wide by approximately 50-meter long test section and an 8m diameter turntable. It is commonly used for simulations of the ABL in wind engineering studies. The wind engineering test section can be configured to give a wide range of turbulence characteristics by changing the screens at the entrance of the

section, combined with changes to the lower part of the tunnel. As well as the conventional method of utilising grids, other changes include varying the nozzle exit elevation and the collector position, see Figure 5. These changes permit the generation of turbulence intensities up to 25% in the wind engineering tests section, with longitudinal integral length scales of up to 1.7m. For the tests described here it was configured to give a longitudinal turbulence intensity of 7.5% and a longitudinal integral length scale of 1.21 m.

D. 2-D and 3-D Test Configurations

A nominally 2-D test configuration utilised a 900mm long version of the aerofoil described above, mounted between end plates with four guying threads, as shown in Figure 4. Pressure measurements were taken at 2 spanwise stations separated by 200mm simultaneously over the wing at 20 chord wise locations. NB results are only presented here for one spanwise location; the second series of taps are being used to investigate spanwise correlations which will be reported elsewhere. No pressure taps were located on the underside of the airfoil for the 2-D configuration; underside pressures were gathered by setting the aerofoil to a negative angle of incidence.

A 300mm span version of the airfoil without end plates was used for the 3-D tests. Fluctuating pressures were measured at midspan using 20 pressure taps each on top and bottom surface of the wing. Due to the need to maintain a large test section area for the generation of turbulence, the wing was mounted in the RMIT Industrial Wind Tunnel in an open-ended configuration supported on the bottom (see Figure 3). A 3-D open ended configuration provided a simpler solution that gives a more realistic representation of a real MAV wing. It was shown that whilst the flow around the wing is inherently 3-D in nature, at the location of the pressure taps the flow is similar to the 2-D case. This was established through the use of flow visualization [8] where it was shown that at the location of the pressure taps there was little influence on the flow structure from the wing tip vortex, and there was minimal spanwise flow. 3-D tests were limited to only the IWT.



Figure 6 – Pressure tapped wing - 3-D configuration mounted on ground plane, RMIT IWT

III. RESULTS AND DISCUSSION

The surface pressure data were processed to give the pressure coefficient (C_p) distribution over the airfoil for each test condition. The time-averaged variation of the pressure

coefficient at different turbulence intensities but with similar integral length scales conditions for 6° angle of incidence is depicted in the figure below.

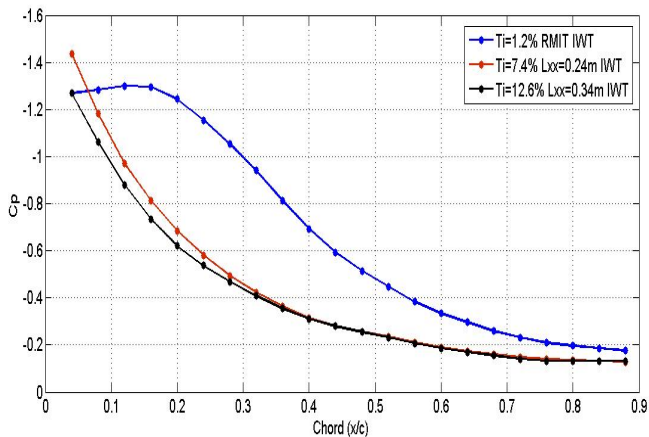


Figure 7 – Pressure coefficient distribution over airfoil at 6° within different levels of turbulence

The length of the laminar separation bubble (LSB) is the region of nominally constant peak Cp at the leading edge of the airfoil. It can be seen from Figure 7 that the length of the bubble reduces significantly with increase in turbulence intensity. The figures below consolidate all Cp distributions as a function of angle of incidence in the different turbulence conditions. Only plots of 3-D wing displayed below; the 2-D results are closely similar.

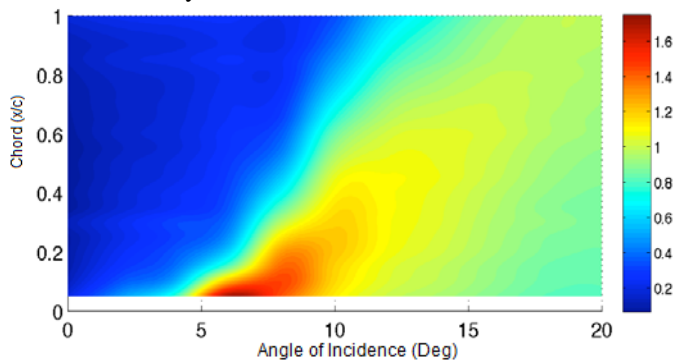


Figure 8 – Consolidated pressure coefficient distribution over 3-D wing in 1.2% turbulence intensity

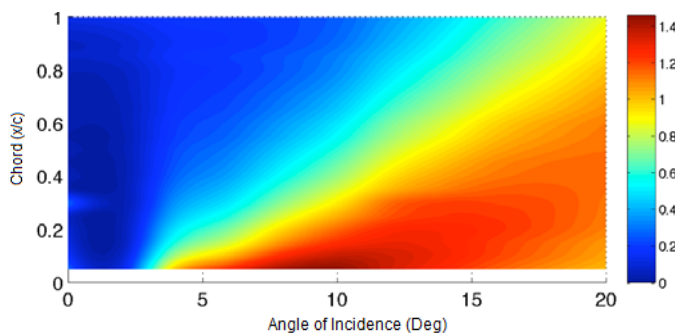


Figure 9 – Consolidated pressure coefficient distribution over 3-D wing in Ti=7.4% and Lxx=0.24m

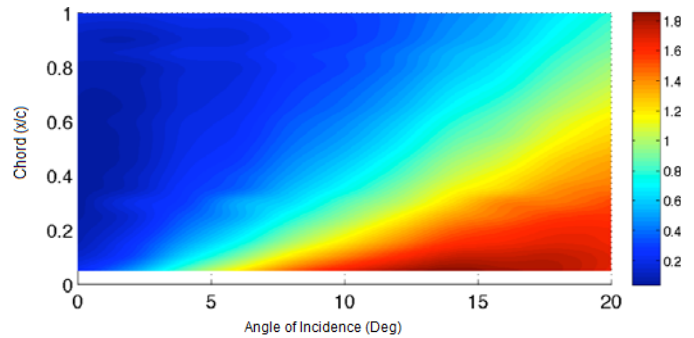


Figure 10 – Consolidated pressure coefficient distribution over 3-D wing in Ti=12.6% and Lxx=0.34m

The enhanced shortening of the LSB along with the increases in angle of incidence at peak lift with increase in turbulence intensity is evident from the plots above. Previous research states that the structure of the LSB is indeed very complex and dynamic. The point of reattachment of the separated shear layer varies with time over the airfoil. The region of max fluctuations in pressure over the airfoil chord indicates the location of reattachment. Figures below show the consolidated standard deviation of pressure at different angles of incidence at different turbulence intensities.

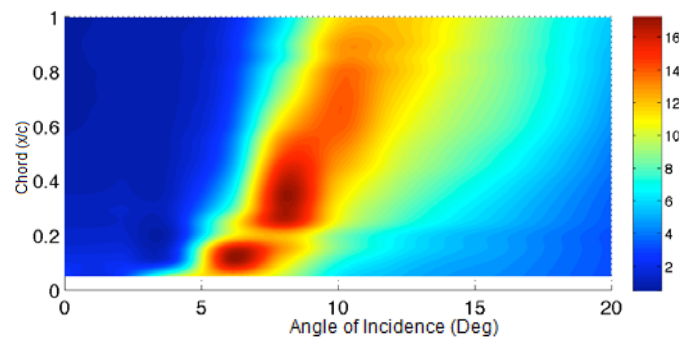


Figure 11 – Standard Deviation of pressure fluctuations over 3D wing when Ti=1.2%

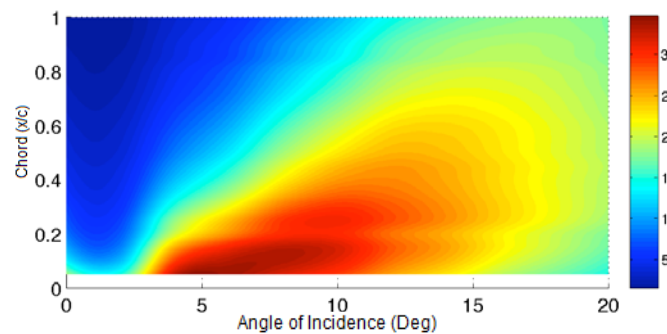


Figure 12 – Standard Deviation of pressure fluctuations over 3D wing when Ti=7.4% and Lxx=0.24m

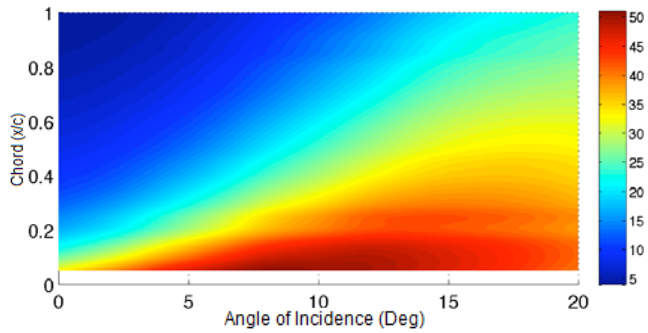


Figure 13 – Standard Deviation of pressure fluctuations over 3D wing when $Ti=12.6\%$ and $L_{xx}=0.34m$

The overall lift coefficients for the 2-D cases were obtained through the integration of the C_p distribution. From the plot below, the influence of the integral length scale and intensity can be identified.

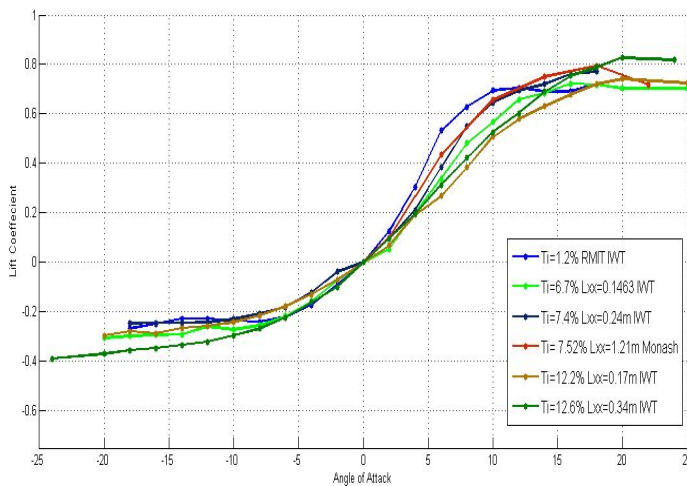


Figure 14 – Suction side C_l Vs angle of incidence plot of airfoil within different turbulence intensities and length scales

From the plots above, it can be inferred that turbulence intensity governs the location of angle of max lift coefficient while the integral length scale governs the gradient of the lift curve slope. An increase in turbulence intensity indicates an increase in the maximum lift coefficient. The angle at which of max lift coefficient is attained remains nominally constant at different length scales with similar intensity. However, as the integral length scale increases, to well beyond the chord length of the airfoil, the lift curve slope is closest to smooth flow condition. This indicates that as integral length scale increases the time averaged airfoil characteristics tend to become similar to steady state condition. The reduction in lift curve slope is believed to be due to the unsettled boundary layer created due to the high energy small turbulence eddies present within small length scale turbulent flows.

The time varying fluctuation of the pressure creates lift fluctuations over the airfoil, this leads to unsteadiness in flight. It is therefore desirable to understand the frequency content of pressure fluctuations. The subsequent spectrograms show the consolidated power spectra density plots for the 3-D cases at 6 degrees angle of incidence with different turbulence conditions.

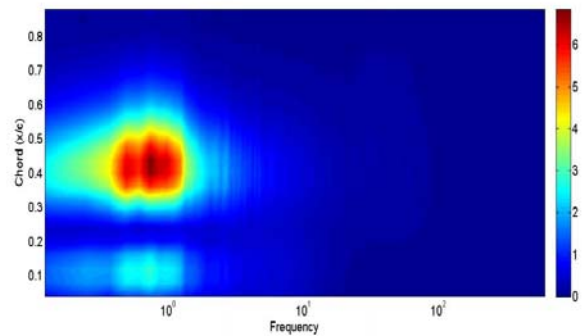


Figure 15 – Power Spectral Density (PSD) of pressure fluctuation over airfoil at 6° angles of incidence when $Ti=1.2\%$

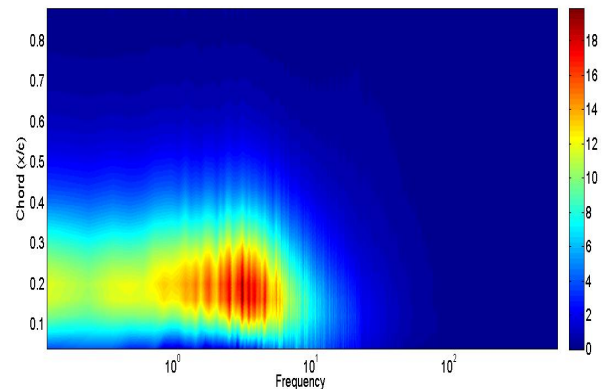


Figure 16 – PSD of pressure fluctuation over airfoil @ 6° angles of incidence when $Ti=7.4\%$ $L_{xx}=0.24m$

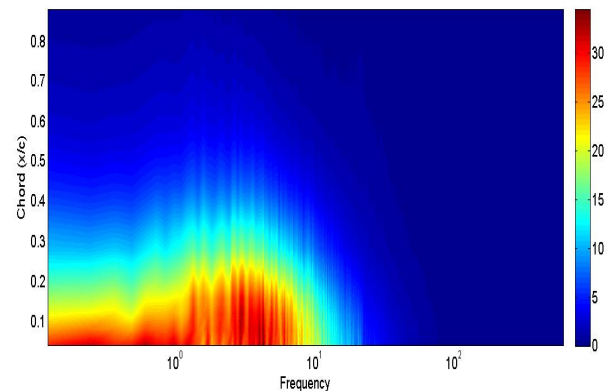


Figure 17 – PSD of pressure fluctuation over airfoil @ 6° angles of incidence when $Ti=12.6\%$ $L_{xx}=0.34m$

In nominally smooth flow condition (Figure 15), there appears to be a periodic fluctuation of pressures at around 0.9 hertz. The location of the maximum power in pressure fluctuation over the airfoil appears to match the point of reattachment of the shear layer. The frequency distribution of pressure fluctuation over the aerofoil in turbulent flow is noticeably different compared to relatively smooth flow. There is a greater spread in the frequencies of oscillation of pressure fluctuation. Frequency at max power of fluctuation also becomes higher i.e. around 4 hertz for both turbulence conditions shown in figures 16 & 17. An increase in power of is also noticed, as can be seen from the color bar on the right of figure 15, 16 & 17. This is due to amplified disturbances present in the shear layer within a turbulent environment.

Periodic pressure fluctuations manifest themselves as lift fluctuations over the wing thus creating rolling and pitching moments when in flight. It is therefore desirable to quantify the rolling and pitching moments experienced by airfoils and wings at different turbulence intensities and length scales. Ongoing research aims to identify these forces and moments over the airfoil. Flow visualization experiments are also going to be conducted in order to elucidate on the structure of the boundary layer over the airfoil.

IV. CONCLUDING REMARKS

The results show that changes in integral length scale and turbulence intensity have significant influence on thin flat-plate aerofoil performance – both dynamically and when data are time-averaged. It seems likely that similar effects will be evident on cambered sections but further work is required to determine this. Since MAVs will fly outdoor in much longer integral length scales than can generated in wind-tunnel studies, it is considered that other methods of testing be considered. This could include tests conducted outdoors during suitable atmospheric conditions. An alternative would be to consider reduced scale dynamic tests as is commonplace in wind engineering; but a drawback of such tests is a compromise on Reynolds number scaling. The work here also raises questions about the nature of 2-D sectional testing in 3-D turbulence – either replicated or simulated. As a solid boundary (e.g. tunnel walls or Earth's surface) is approached it is known that the turbulence changes characteristics, with the cross-plane intensity being forced to zero at the boundary and changes in the longitudinal and transverse length scales. Since MAVs tend to have very low aspect ratios, it might be useful to consider a standard (low) aspect ratio for 3-D testing to further understand the nature of turbulence on both time-averaged and dynamic effects. The understanding of such effects is part of our continuing research.

ACKNOWLEDGMENT

The authors would like to acknowledge the assistance of the technical staff at RMIT and Monash Universities.

REFERENCES

- [1] Anon (1997) 'UAVs Applications are Driving Technology – Micro Air Vehicles', UAV Annual Report, Defense Airborne Reconnaissance Office, Pentagon, Washington, 6 November, p.32.
- [2] Spedding, G.R., and Lissaman, P.B.S., "Technical Aspects of Microscale Flight Systems", *Journal of Avian Biology*, Vol. 29, No. 4, 1998, pp.458-468.
- [3] Pines, DJ., Bohorquez, F. "Challenges Facing Future Micro-Air-Vehicle Development", *Journal of Aircraft*, Vol 43, No. 2 March 2006 pp 290-305.
- [4] Mueller, T. J., "Aerodynamic Measurements at Low Reynolds Numbers for Fixed Wing Micro-Air Vehicles", RTO AVT/VKI Special Course on Development and Operation of UAVs for Military and Civil Applications, September 13-17, 1999, VKI, Belgium.
- [5] Watkins S., Milbank J., Loxton B., Melbourne W., "Atmospheric Winds and their Effects on Micro Air Vehicles" *AIAA Journal*, 2006.
- [6] Watkins S., Abdulrahim M., Thompson M., Shortis M., Segal R. and Sheridan J., "An Overview of Experiments on the Dynamic Sensitivity of MAVs to Turbulence", *Journal of the Royal Aeronautical Society*, accepted for publication 25th March 2010.
- [7] Turbulent Flow Instrumentation website in which the DPMS pressure measurement system is detailed, see: <http://www.turbulentflow.com.au>.
- [8] Loxton B., Watkins S., Watmuff J., Trivalio P., Cruz E., Ravi S., "The Influence of Atmospheric Turbulence on the Aerodynamics of a Flat Plate Micro Air Vehicle Wing", 3rd Australasian Unmanned Air Vehicles Conference, 9 - 12 March, 2009, Melbourne, Australia
- [9] Watkins S., Loxton B., Milbank J., Melbourne W. H. and Abdulrahim M. "Modelling the Atmospheric Boundary Layer in a Large Wind Tunnel for MAV Development" 46th AIAA Aerospace Sciences Meeting and Exhibit, 7-10 Jan. 2008, Reno NV USA.